Journal of Alloys and Compounds 509 (2011) 1691–1695

Contents lists available at ScienceDirect

Journal of Alloys and Compounds

journal homepage: www.elsevier.com/locate/jallcom

Micro-indentation study of Mg-addition MgB_2 superconducting wires

N. Güçlü *

Department of Physics, Faculty of Science and Arts, Gaziosmanpaşa University, 60240 Tokat, Turkey

ARTICLE INFO

Article history:
Received 9 April 2010
Received in revised form
25 September 2010
Accepted 28 September 2010
Available online 8 October 2010

PACS:
74.70Ad
74.25Ld

Keywords:
MgB_2 wire
Mg-added
Hardness
Elastic modulus

ABSTRACT

The Mg-added (0%, 5%, and 10%) MgB_2/Cu superconducting wires were prepared by the powder-in-tube (PIT) method. Vickers micro-indentation tests were performed on the samples with different peak loads at room temperature. The loading–unloading (P–h) curves were analyzed by the displacement approach to indentation. It was found that hardness (H) and the effective elastic modulus (E) values increased with Mg-added. In addition, these values showed peak load dependence (i.e. indentation size effect (ISE)).

1. Introduction

Since the discovery of superconductivity in MgB_2 [1], many efforts have been made to improve the properties of MgB_2 by doping and/or adding and changing conditions of sample preparation [2–6]. The improvement of the superconducting properties of the sample is a decisive goal to enable its potential application. The compound has been found to be attractive given the possibility that it can be its relatively high transition temperature, high transport critical current density, large coherence length, simple crystal structure and the low cost of materials. These features make it a promising candidate for applications in the field of high-field magnets, power-transmission cables, transformers, motors, generations and current leads at temperature above 20 K. According to liquid helium temperature, the temperature (>20 K) obtained is dramatically cheaper and requires less sophistic and less onerous cryogenic equipments. These applications require the development of MgB_2 wires and tapes with superior transport current carrying capacities under external magnetic fields that requires diversified fabrication techniques. The powder-in-tube (PIT) method has been a common commercial technique of producing wires and tapes from brittle superconductor. In this method, the brittle superconducting power is filled into a ductile metal tube and then swaged into small diameters for various applications. The method has been widely used for both conventional superconductors and HTS [7]. Several groups have fabricated MgB_2 wires or tapes with high critical current density using the PIT method [8,9]. On the other hand, the grain size of MgB_2 is an important factor for grain connectivity in these superconducting wires. Poor connectivity between grains and lack of pinning centres are the cause of low critical current densities in these wires. In the literature, many attempts have been made to improve the pining properties and J_c of MgB_2 wires by methods such as elemental addition or doping (Ti, Al, and Zr) [10], lauric acid doping [11], polymethyl-methacrylate doping [12], and O-free polyacrylonitrile doping [13]. It is expected that the mechanical properties were improved with the aforementioned experiment techniques. Therefore, in previous works [14], MgB_2 and Ti-added MgB_2 superconducting wires are characterized using a dynamic ultra-microindentation experimental technique. We found that hardness and elastic modulus increased with added Ti. In addition, these values showed peak load dependence (i.e. indentation size effect (ISE)). To our knowledge, no detailed study on the mechanical properties of Mg-added MgB_2 wire has been published in the literature.

Depth-sensing indentation is widely used to assess the mechanical properties of materials, such as their hardness and elastic modulus. This method is preferred because relatively small amounts of testing material are needed and there are no strict requirements for the shape of the sample. In addition, the measurements can be performed without the destruction of the sample. The

* Tel.: +90 356 252 15 82x3055; fax: +90 356 252 15 85.
E-mail address: guclu06@hotmail.com

0925-8388/$ – see front matter © 2010 Elsevier B.V. All rights reserved.
doi:10.1016/j.jallcom.2010.09.178

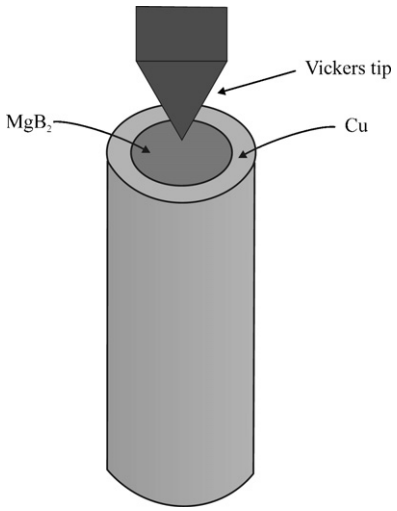

Fig. 1. Schematic illustration of indentation experiment on wire.

most important measurements given by a depth-sensing indentation test are the indentation load P and penetration depth h. Many methods are developed in the literature to analyze the P–h curves [15,16]. However, these methods may not be reliable when the pile-up or sink-in behaviours occur. The work of indentation approach and the displacement approach to indentation is both applicable to the cases of pile-up and the sink-in and do not require imaging of the residual indents. The work of indentation approach was first proposed by Stillwell and Tabor [17]. Then, Sakai [18] put forward a relationship between the energy of the hysteresis indentation loop and the hardness. Recently, Attaf [19] has also used the work of indentation approach to suggest some material constants. The displacement approach to indentation was developed by Giannakopoulos and Suresh [20]. They showed that the two methods (i.e. the work of indentation approach and the displacement approach to indentation) are equivalent to each other.

In this paper, we characterized the mechanical properties of Mg-added MgB_2 superconducting wires at room temperature using a dynamic ultra-microindentation experimental technique. To calculate the hardness and effective elastic modulus values, the loading–unloading (P–h) curves were analyzed by the displacement approach to indentation of Giannakopoulos and Suresh [20]. We noted that these values increased with added Mg.

2. Experimental

The Mg-added (0%, 5%, and 10%) MgB_2/Cu superconducting wires were prepared by the PIT method. The preparation details, structure and superconductivity properties are described in the work of Okur et al. [21]. A Vickers indenter was used in a dynamic ultra microhardness tester (Shimadzu, DUH-W201S). The indenter was operated axially at the centre of the wire as shown in Fig. 1. The experiments were performed on the samples after they had been annealed at 400 °C for 2 h. All tests were performed under the same operating conditions to avoid uncertainties arising from changes in the experimental procedure. The experiments were carried out at different peak loads with loading rate of 14.12 mN/s.

3. Theoretical consideration

Fig. 2 shows a typical load–penetration depth curve which includes both the loading and unloading data for a general viscoelastic plastic material. The data obtained from the unloading curve provide information regarding the elastic, viscoelastic and plastic behaviour. The important quantities are the peak load (P_{max}), the maximum depth (h_{max}), and the final depth (h_f).

Accurate measurement of the contact area (A_{max}) is critical to the measurement of the hardness and elastic modulus by microindentation. This is particularly important since the contact area

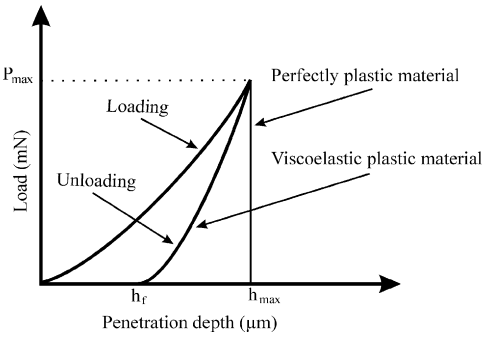

Fig. 2. Typical indentation cycles showing load–unload curves.

may be overestimated if material sink-in takes place at the edges of the indentation. Fig. 3 shows schematic illustrations of sink-in around a sharp indenter. Giannakopoulos and Suresh [20] examined this problem using three-dimensional simulations.

Parameter S is related to the ratio of h_f to h_{max} by [20]

$$\frac{h_f}{h_{max}} = 1 - d^*S \tag{1}$$

where $d^* = 5$ for the Vickers pyramid indenter. Using the value of h_f/h_{max} (Table 1), the S values are calculated by Eq. (1). Obtained values of S is put into Eq. (2) and then the contact area (A_{max}) is calculated from [20]

$$\frac{A_{max}}{h_{max}^2} = 9.96 - 12.64(1-S) + 105.42(1-S)^2 - 229.57(1-S)^3 + 157.67(1-S)^4 \tag{2}$$

Hardness is defined using the contact area values estimated in Eq. (2)

$$H = \frac{P_{max}}{A_{max}} \tag{3}$$

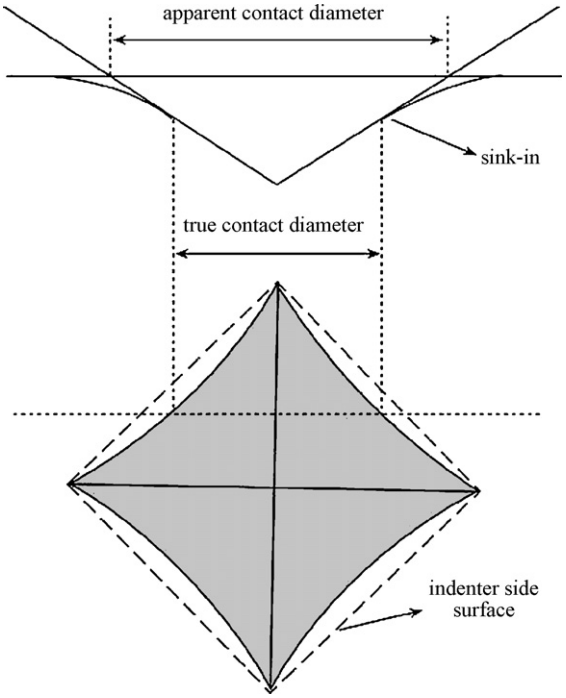

Fig. 3. Schematic illustration of sink-in around a sharp indenter [20].

Table 1
Experimental data of the final depth, the maximum depth and the ratio of h_f/h_{max}.

Sample	P_{max} (mN)	h_{max} (μm)	h_f (μm)	h_f/h_{max}
0% Mg-added MgB_2 wire	50	0.49	0.36	0.74
	100	0.89	0.50	0.56
	150	1.27	0.78	0.61
	200	1.62	0.97	0.60
	250	1.97	1.18	0.60
	300	2.33	1.42	0.61
	350	2.63	1.64	0.62
	400	2.90	1.86	0.64
5% Mg-added MgB_2 wire	50	0.50	0.39	0.78
	100	0.78	0.55	0.71
	150	1.00	0.67	0.67
	200	1.22	0.80	0.66
	250	1.41	0.91	0.65
	300	1.61	1.04	0.65
	350	1.79	1.14	0.64
	400	1.95	1.26	0.65
10% Mg-added MgB_2 wire	50	0.42	0.34	0.81
	100	0.68	0.49	0.72
	150	0.88	0.60	0.68
	200	1.05	0.71	0.68
	250	1.21	0.80	0.66
	300	1.36	0.88	0.65
	350	1.49	0.96	0.64
	400	1.63	1.04	0.64

The ratio of H and S is now known as

$$E = \frac{H}{S} \tag{4}$$

where E is the effective elastic modulus.

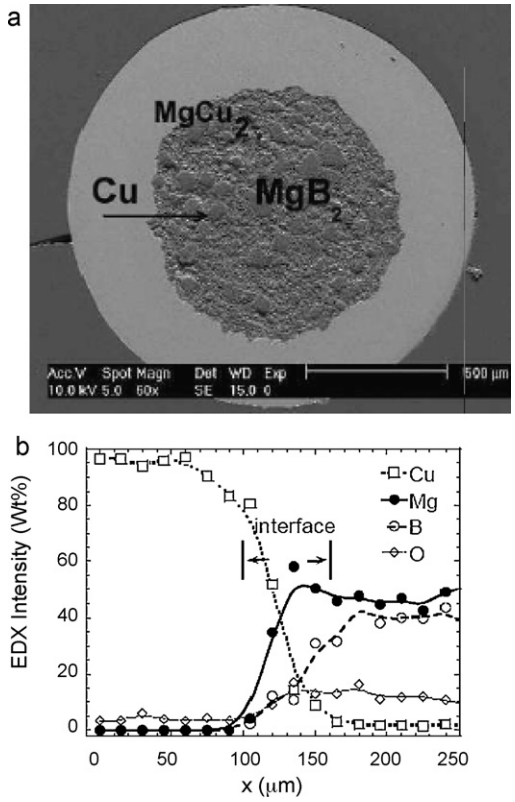

Fig. 4. (a) SEM picture of a 5% Mg added Cu clad MgB_2 superconducting composite wire [21]. (b) EDX Intensity taken at the interface between Cu sheath and MgB_2 + 5% Mg core while moving in a direction from along the radial towards the core centre as shown in (a) [21].

4. Results and discussion

The SEM picture of 5% Mg added to Cu clad MgB_2 superconducting composite wire is given in Fig. 4a after annealing. The diameter of the composite core in the SEM picture was measured to be about 0.8 mm and outer diameter 1.5 mm. Fig. 4b shows EDX intensity taken at the interface between the Cu sheath and MgB_2/Mg core while moving from the Cu sheath to the MgB_2 + 5% Mg superconducting core about 250 μm along the radial direction as marked in Fig. 4a. In the interface region (from 100 μm to 150 μm), the rations of Cu decrease and Mg and B start to increase. It is noticed that the stoichiometry of MgB_2 is not maintained and excess Mg and Cu are more pronounced. Furthermore, inside the superconducting core the Mg and B ratio is close to the MgB_2 stoichiometry [21].

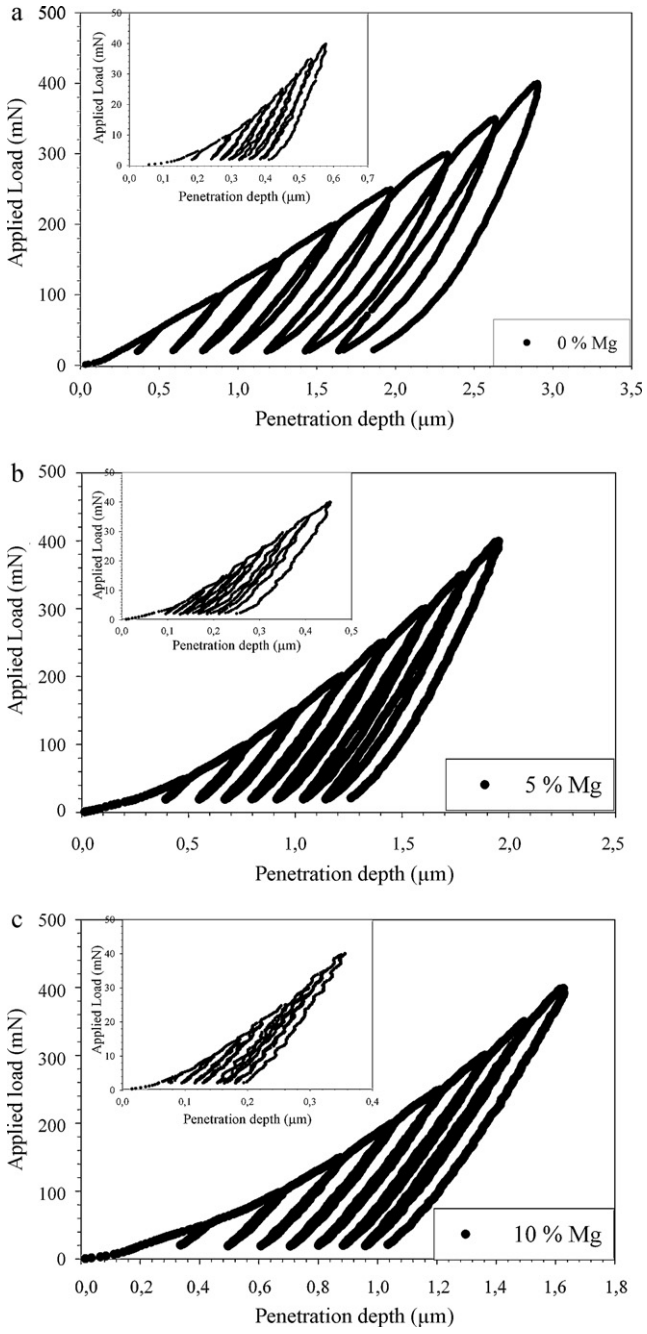

Fig. 5. Load–penetration depth behaviour of MgB_2 composite wire at room temperature. (a) Pure MgB_2 wire, (b) 5% Mg-added MgB_2 wire, and (c) 10% Mg-added MgB_2 wire.

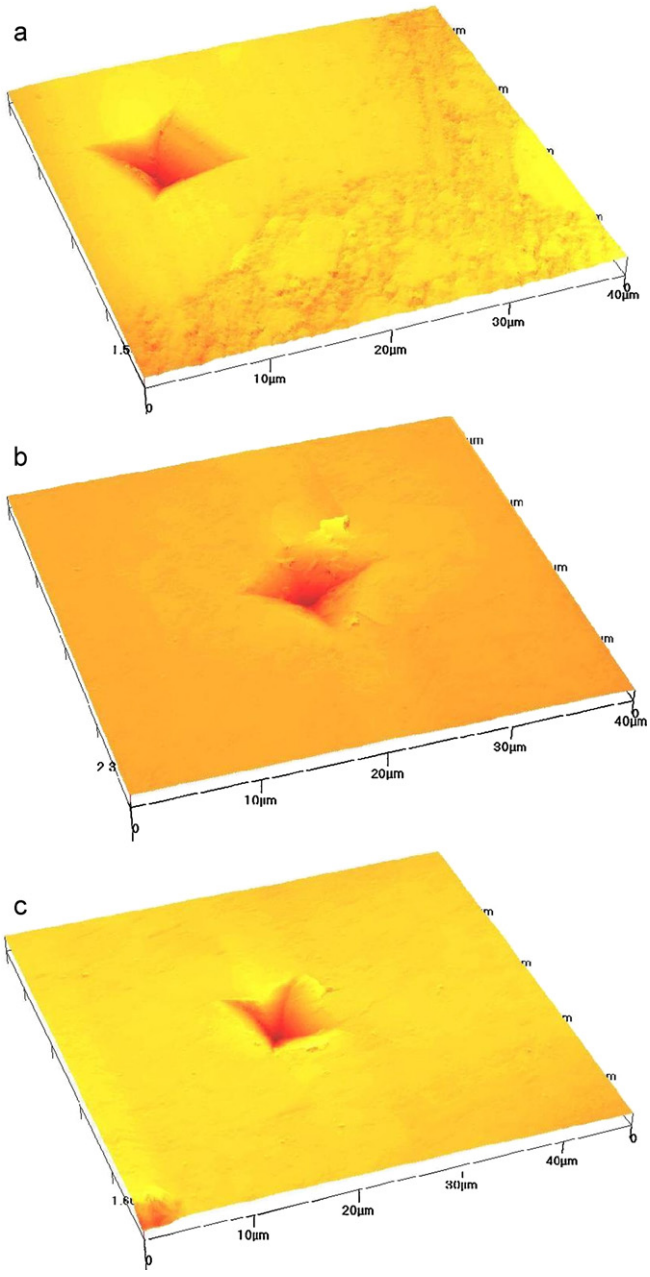

Fig. 6. AFM micrograph of residual impression after indentation experiment. (a) Pure MgB_2 wire, (b) 5% Mg-added MgB_2 wire, and (c) 10% Mg-added MgB_2 wire.

Fig. 5 is a typical load–penetration depth curve for micro-indentation. The depth-sensing indentation tests were conducted at three samples (0% Mg (a), 5% Mg (b), 10% Mg (c)), with different peak loads at room temperature. The inset plot in the figures indicates a lower load–penetration depth curve. The curves demonstrated that all samples show both elastic and plastic deformations during Vickers indentation. It is clearly seen that penetration depths with the same peak loads decrease due to added Mg. These results imply that the hardness of MgB_2 values increased with added Mg. On the other hand, according to Fig. 4a [21], T_c^{Onset} of the Mg-added 5% and 10% MgB_2 are 32 K and 34 K, respectively. It is observed that the increasing Mg content slightly raises the critical temperatures of the samples. This result is also similar to the work of Eğilmez et al. [7].

The key experimentally measurable parameter used to identify the expected indentation behaviour of a given material is the ratio

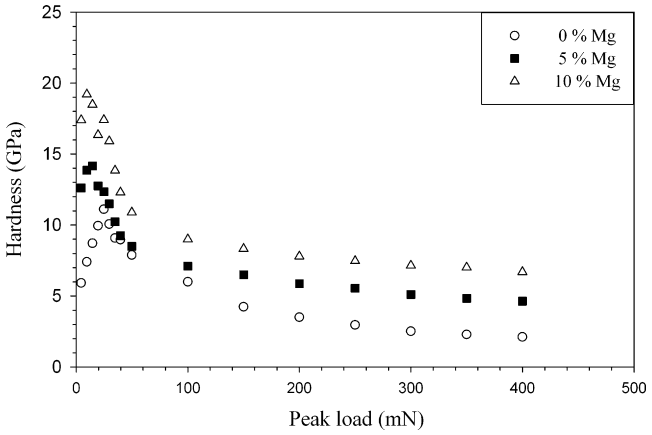

Fig. 7. Variation of the hardness with the peak load.

of final indentation depth, h_f, to the depth of the indentation at peak load, h_{max} [20]. Note that the ratio h_f/h_{max} can be extracted from the unloading curve in a microindentation experiment. In addition, since the Vickers indenter has self-similar geometries, h_f/h_{max} does not depend on the depth of indentation. The natural limits for the parameter are $0 \leq h_f/h_{max} \leq 1$. The lower limit corresponds to full elastic deformation, whereas the upper limit corresponds to rigid-plastic behaviour. A critical value is generally taken as 0.875, which is the boundary between pile-up (values >0.875) and sink-in (values <0.875) [20]. Values in the "sink-in" range imply work-hardening behaviour. The h_f/h_{max} values are listed in Table 1 for our samples. The ratios of h_f/h_{max} at different applied loads are lower than the critical value. These results show that sink-in is dominant in our samples. This result is also supported by the AFM micrograph of the samples in Fig. 6.

The mechanical properties measured most frequently using load and depth sensing indentation techniques are the hardness, H and the elastic modulus, E. In a commonly used method, data are obtained from one complete cycle of loading and unloading. Since the sink-in is dominant in our samples, hardness and effective elastic modulus are calculated by the displacement approach to indentation [20]. The hardness values for three samples have been plotted as a function of peak load (Fig. 7). If we look at the hardness values, we find that the hardness values increases at the lower peak load. This kind of behaviour shown in Fig. 7 is called indentation size effect (ISE) [16,22]. The hardness increases with added Mg. The increasing of hardness values is associated with reduction of the porosity within the composite structure and a better compaction of the MgB_2 powders due to the presence of the Mg metal

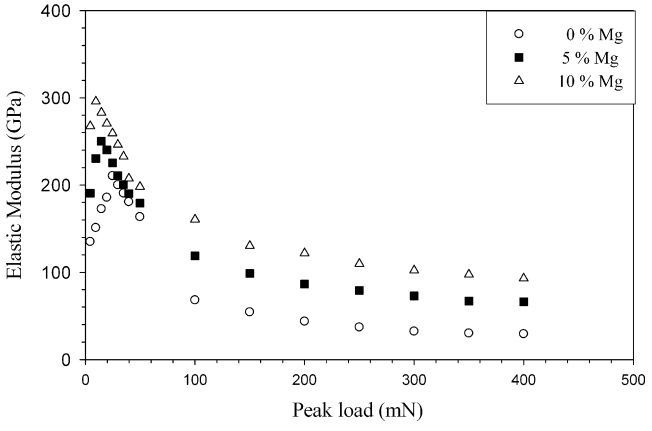

Fig. 8. Variation of the effective elastic modulus with the peak load.

[7]. On the other hand, $\overline{P}$ is the average applied load in the vicinity of zero load. In this phenomenon, the value of $\overline{P}$ takes 25, 15, 10 mN for 0%, 5% and 10% Mg-added MgB_2 wires, respectively. The adding rate increases as the value of $\overline{P}$ decreases (Fig. 7). In addition, the maximum hardness (H_{max}) increases as the adding rate increases. In general, this result is similar to that of Ti-added MgB_2 wires [14].

Fig. 8 shows the effective elastic modulus versus peak load. Like hardness, effective elastic modulus increases with Mg-added and also increases with decreasing peak load. This result is similar to that of Ti-added MgB_2 wires and MgB_2/Mg composites [14]. The hardness and modulus of Mg-added MgB_2 wires are also compared with the literature [23] ranging from 10.12 to 17.10 and from 213 to 273 GPa of bulk MgB_2 sample, respectively.

5. Conclusions

The Mg-added (0%, 5%, and 10%) MgB_2/Cu wires were investigated using a dynamic ultra-microindentation experimental technique. The ratios of h_f/h_{max}, lower than the critical value (0.875) at various peak loads, imply sink-in and work hardening behaviour in our samples. Hardness and effective elastic modulus values are calculated by the displacement approach to indentation. It is found that the values increase with Mg-added and exhibit significant peak load dependence (i.e., indentation size effect (ISE)).

Acknowledgement

The author is thankful to Dr. S. Okur at Izmir Institute of Technology for the supply of the samples.

References

[1] J. Nagamatsu, N. Nakagawa, T. Muranaka, Y. Zenitani, J. Akimitsu, Nature 410 (2001) 63–64.
[2] A. Matsumoto, H. Kitaguchi, H. Kumakura, Physica C 470 (2010) 1446–1449;
C.H. Cheng, Y. Yang, C. Ke, H.T. Lin, Physica C 470 (2010) 1092–1095.
[3] S.K. Chen, X. Xu, J.H. Kim, S.X. Dou, J.L. MacManus-Driscoll, Physica C 470 (2010) 1211–1215;
M. Ranot, S.-G. Jung, W.K. Seong, N.H. Lee, W.N. Kang, J. Joo, C.-J. Kim, B.-H. Jun, S. Oh, Physica C (in press).
[4] K.J. Song, C. Park, S. Kang, Physica C 470 (2010) 470–474;
S. Zhou, S. Dou, Solid State Sci. 12 (2010) 105–110.
[5] P.C. Canfield, D.K. Finnemore, S.L. Budko, Phys. Rev. Lett. 86 (2001) 2423–2426;
B.A. Glowacki, M. Majoros, M. Vickers, J.E. Evetts, Y. Shi, I. McDougall, Supercond. Sci. Technol. 14 (2001) 193–199.
[6] E. Yanmaz, K. Ozturk, C.E.J. Dancer, M. Basoglu, S. Çelik, C.R.M. Grovenor, J. Alloys Compd. 492 (2010) 48–51;
B-.H. Jun, N.-K. Kim, K.S. Tan, C.-J. Kim, J. Alloys Compd. 492 (2010) 446–451.
[7] M. Eğilmez, L. Ozyuzer, M. Tanoglu, S. Okur, O. Kamer, Y. Oner, Supercond. Sci. Technol. 19 (2006) 359–364.
[8] A. Kılıç, S. Okur, N. Güçlü, U. Kölemen, O. Uzun, L. Özyüzer, A. Gencer, Physica C 415 (2004) 51–56;
K. Yamamoto, K. Osamura, S. Balamurugan, T. Nakamura, T. Hoshino, I. Muta, Supercond. Sci. Technol. 16 (2003) 1052–1058.
[9] G. Alecu, V. Adlıca, A. Vonıa, S. Hodorogea, J. Optoelect. Adv. Mater. 10 (2008) 2981–2984.
[10] W.J. Feng, S. Zhang, Y.Q. Guo, H. Yang, T.D. Xia, Z.Q. Wei, Physica C 470 (2010) 236–239;
J.Y. Xiang, D.N. Zheng, J.Q. Li, S.L. Li, H.H. Wen, Z.X. Zhao, Physica C 386 (2003) 611–615;
Y. Zhao, F. Feng, D.X.T. Machi, C.H. Cheng, K. Nakao, N. Chikumoto, Physica C 378–381 (2002) 122–126.
[11] C.M. Lee, S.M. Lee, G.C. Park, J. Joo, J.H. Lim, W.N. Kang, J.H. Yi, B.-H. Jun, C.-J. Kim, Physica C 470 (2010) 1438–1441.
[12] G.C. Park, S.M. Hawang, C.M. Lee, J.H. Choi, J. Joo, J.H. Lim, W.N. Kang, C.-J. Kimi, Physica C (in press).
[13] S.M. Hwang, K. Sung, J.H. Choi, W. Kim, J. Joo, J.H. Lim, C.-J. Kim, Y.S. Park, D.H. Kim, Physica C 470 (2010) 1430–1434.
[14] N. Güçlü, O. Uzun, U. Kölemen, Mater. Character 57 (2006) 166–170;
N. Güçlü, Mater. Chem. Phys. 101 (2007) 470–474.
[15] W.C. Oliver, G.M. Pharr, J. Mater. Res. 7 (1992) 1564–1583.
[16] K. Sangwal, Cryst. Res. Technol. 44 (2009) 1019–1037;
N.K. Mukhopadhyay, P. Paufler, Int. Mater. Rev. 51 (2006) 209–245.
[17] N.A. Stillwell, D. Tabor, Proc. Phys. Soc. Lond. 78 (1961) 169–179.
[18] M. Sakai, Acta Metall. Mater. 41 (1993) 1751–1758.
[19] M.T. Attaf, Mater. Lett. 57 (2003) 4684–4693.
[20] A.E. Giannakopoulos, S. Suresh, Scr. Mater. 40 (1999) 1191–1198.
[21] S. Okur, M. Kalkanci, M. Yavas, M. Eğilmez, L. Ozyuzer, J. Optoelect. Adv. Mater. 7 (2005) 411–414.
[22] C. Terzioglu, A. Varilci, I. Belenli, J. Alloys Compd. 1–2 (2009) 836–841;
U. Kölemen, J. Alloys Compd. 425 (2006) 429–435;
O. Uzun, U. Kölemen, S. Çelebi, N. Güçlü, J. Eur. Ceram. Soc. 25 (2005) 969–977.
[23] T.A. Prikhna, ArXiv.0912.4606 (2009).;
T.A. Prikhna, ArXiv.0204362 (2002).